Using recurrences to characterize the hyperchaos-chaos transition

Everton G. Souza, Ricardo L. Viana,* and Sérgio R. Lopes
Departamento de Física, Universidade Federal do Paraná, 81531-990, Curitiba, Paraná, Brazil
(Received 1 April 2008; published 10 December 2008)

Hyperchaos occurs in a dynamical system with more than one positive Lyapunov exponent. When the equations governing the time evolution of the dynamical system are known, the transition from chaos to hyperchaos can be readily obtained when the second largest Lyapunov exponent crosses zero. If the only information available on the system is a time series, however, such method is difficult to apply. We propose the use of recurrence quantification analysis of a time series to characterize the chaos-hyperchaos transition. We present results obtained from recurrence plots of coupled chaotic piecewise-linear maps and Chua-Matsumoto circuits, but the method can be applied as well to other systems, even when one does not know their dynamical equations.

DOI: 10.1103/PhysRevE.78.066206 PACS number(s): 05.45.Ra, 05.45.Jn, 05.45.Xt

I. INTRODUCTION

Hyperchaotic attractors have at least two positive Lyapunov exponents [1], and hyperchaos is expected to be rather ubiquitous in higher-dimensional systems like coupled oscillators and maps [2]. Moreover, hyperchaotic behavior has been experimentally observed in electronic circuits [3], NMR lasers [4], *p*-Ge semiconductor systems [5], and chemical reactions [6]. When the equations governing the time evolution of the dynamical system are known (either in continuous or discrete time) the chaos-hyperchaos transition can be investigated as a system parameter is varied so as to reach a critical value, for which the second largest Lyapunov exponent, λ_2, crosses zero [7]. On the other hand, if the dynamical equations are not known *a priori*, as it is often the case in a physical experiment, the task of determining the chaos-hyperchaos transition becomes considerably more difficult.

Let us first imagine that one tries to use delay coordinates and a phase-space embedding from a single scalar time series of the system under study, using a measurement function $h:R^d \mapsto R^m$ [8]. Since the minimal phase-space dimension for observing a hyperchaotic attractor is four (for a continuous system), the embedding process introduces spurious foldings. The projection of a hyperchaotic attractor in R^d onto R thus results in false neighbors which cannot be generally removed by increasing the embedding dimension d [9]. Another problem related to the embedding of hyperchaotic attractors occurs when the largest Lyapunov exponents are such that λ_1 is sufficiently larger than $\lambda_2 > 0$. In this case, measurements made a long time ago are not relevant to the present state of the system, such that the reconstructed attractor diverges exponentially as the embedding dimension d [10].

On account of the many problems that arise when the chaos-hyperchaos transition is investigated in systems where only a single scalar time series is available, it would be useful to exploit other dynamical characterizations. In this paper we propose the use of recurrences to investigate the parameter value where the chaos-hyperchaos transition occurs in a system, given only a univariate time series from which one can make a d-dimensional embedding using the vectors $\mathbf{x}_i = \{x_i, x_{i+\tau}, x_{i+2\tau}, \ldots, x_{i+(d-1)\tau}\}$, where τ is the delay [11].

Recurrence plots (RPs) are two-dimensional graphical representations of the matrix [12–14] $\mathbf{R}_{i,j} = \Theta(\epsilon - \|\mathbf{x}_i - \mathbf{x}_j\|)$, $i,j = 1,2,\ldots,N$, where $\mathbf{x}_i \in \mathbb{R}^d$ represents the reconstructed dynamical state at time i, ϵ is a predetermined threshold, $\Theta(\cdots)$ is the unit step function, and $\|\cdots\|$ stands for the Euclidean norm, and N is the total number of points. The RP is thus obtained by assigning a black (white) dot to the points for which $\mathbf{R}_{i,j} = 1$ (0) [10,12].

Recurrence quantification analysis (RQA) consists of a series of measures obtained from a RP which can elucidate various aspects of the system behavior [15]. As an example, stationary time series yield RPs which are homogeneous along a diagonal line. Moreover, if the RP shows a cloud of points with a homogeneous yet irregular distribution, then the time series has a pronounced stochastic nature. On the other hand, the formation of patterns in RPs may indicate stationary chaotic behavior, allowing the computation of dynamical invariants, such as the second-order Rényi entropy and correlation dimension [16,17].

The key idea of this paper is that RQA furnish signatures for the chaos-hyperchaos transition. We use a paradigmatic example, a system of coupled chaotic maps, for which this transition can be readily investigated using the conventional approach, such that it is possible to compare the results with those obtained from RQA. Moreover, as an example of a chaotic system of physical interest we considered a system of two coupled Chua-Matsumoto circuits, where the transition from hyperchaos to chaos have been described from the corresponding Lyapunov spectrum [18]. The recurrence-based diagnostics we consider show that, after the transition from a hyperchaotic to a chaotic attractor, there is a marked increase in our ability to quantify the deterministic content of the time series. This allows recurrence-based diagnostics to be applied to detect this transition in time series from experimental systems, where we barely have a prior knowledge of the governing dynamical equations.

The paper is organized as follows: In the second section we briefly describe the RQA numerical diagnostics used to analyze the time series. Section III analyzes systems of

*Corresponding author; viana@fisica.ufpr.br

coupled chaotic maps as examples of systems undergoing chaos-hyperchaos transitions from the Lyapunov spectrum point of view. Section IV outlines our results for the chaos-hyperchaos transition in systems of coupled chaotic maps using recurrence quantification analysis. Section V presents an application to coupled Chua-Matsumoto circuits. The last section contains our conclusions.

II. RECURRENCE QUANTIFICATION ANALYSIS

In the framework of RQA we have a number of quantitative diagnostics of the distribution of points in a RP, forming there are three basic kinds of structures [14]. The first kind is single, or isolated points, which occur if the dynamical states are rare, do not persist for any time, or fluctuate heavily. The recurrence rate (R_r) is the probability of finding a black recurrence point (for which $\mathbf{R}_{i,j}=1$), or

$$R_r = \frac{1}{N^2} \sum_{i,j=1;i\neq j}^{N} \mathbf{R}_{i,j}, \tag{1}$$

where N^2 is the total number of pixels (black or white) in a RP. We remark that the main diagonal points are excluded from the double sum, since each point is recurrent with itself.

Diagonal lines are structures in a RP parallel to the main diagonal $R_{i,i}=1$, $i=1,2,\ldots,N$, and defined as

$$\mathbf{R}_{i+k,j+k} = 1 \quad (j = 1,2,\cdots N; k = 1,2,\cdots,\ell),$$

$$\mathbf{R}_{i,j} = \mathbf{R}_{i+\ell+1,j+\ell+1} = 0, \tag{2}$$

where ℓ is the length of the diagonal line, which occurs when a segment of a given trajectory (in phase space) runs parallel to another segment. In other words, when a RP presents a diagonal line, two pieces of a trajectory undergo for a certain time (the length of the diagonal) a similar evolution and visit the same region of phase space at different times. This is the key idea of recurrence and thus a clearcut signature of determinism. Accordingly, we compute $P(\ell)=\{\ell_i;i=1,2,\ldots N_\ell\}$, which is the frequency distribution of the lengths ℓ_i of diagonal lines, and N_ℓ is the absolute number of diagonal lines, with the exception of the main diagonal line which always exists by construction.

The determinism is defined as

$$D = \frac{\sum_{\ell=\ell_{\min}}^{\ell_{\max}} \ell P(\ell)}{\sum_{i,j=1,i\neq j}^{N} \mathbf{R}_{i,j}}, \tag{3}$$

where $\ell_{\min}=2$ is the minimum length allowed for a diagonal line, whereas the maximum diagonal length is $\ell_{\max}=\max(\{\ell_i,i=1,2,\ldots N_\ell\})$. Thus, the determinism measures the percentage of points in a RP belonging to diagonal lines. Other related quantities are the ratio between D and R_r and the average diagonal length,

$$L = \frac{\sum_{\ell=\ell_{\min}}^{\ell_{\max}} \ell P(\ell)}{\sum_{\ell=\ell_{\min}}^{\ell_{\max}} P(\ell)}. \tag{4}$$

Following Eckmann *et al.* [12] the lengths of the diagonal lines are related to the inverse of the largest positive Lyapunov exponent of the system. Likewise, the divergence $1/\ell_{\max}$ is related with the Kolmogorov-Sinai (KS) entropy of a dynamical system, or the sum of its positive Lyapunov exponents.

III. CHAOS-HYPERCHAOS TRANSITION IN CHAOTIC COUPLED MAPS

Coupled one-dimensional maps are a natural choice for studying the chaos-hyperchaos transition, since the dynamics of each uncoupled map may be chosen to be simple enough to allow an analytical approach, even when the maps become coupled. This is the case, for example, of piecewise linear maps $x\mapsto f(x)=\beta x(\mathrm{mod}\ 1)$ which, for $\beta>1$, exhibit strong (transitive) chaos [19].

Let us consider first, for the sake of generality, a system of N globally coupled piecewise-linear maps, for which all maps are coupled with each other, regardless of their mutual distance in a one-dimensional lattice,

$$x_{n+1}(i) = f(x_n(i)) + \frac{K}{N} \sum_{j=1,j\neq i}^{N} f(x_n(j)) \quad (i = 1,2,\cdots,N), \tag{5}$$

where $f(x)=\beta x$ and the mod 1 operation is performed after the application of Eq. (5) in order to keep the variable x in the interval [0, 1]. In other words, each map is coupled with the "mean field" of all the other maps with variable strength $K>0$. This is a system extensively investigated, especially due to its applications to neural networks [20].

The special form of coupling expressed by Eq. (5) enables us to obtain some analytical results on the dynamics of the coupled map system, like its Lyapunov spectrum and Kolmogorov-Sinai entropy [21]. The former is comprised by N Lyapunov exponents given by

$$\lambda_1 = \ln \beta, \tag{6}$$

$$\lambda_j = \ln \left| \beta \left[1 - K\left(1 + \frac{1}{N-1} \right) \right] \right| \quad (j = 2,3,\cdots,N), \tag{7}$$

i.e., the Lyapunov spectrum is $(N-1)$-fold degenerate. For $\beta>1$ the system is chaotic since $\lambda_1>0$, and hyperchaotic for $\lambda_j>0$. Hence the hyperchaos-chaos transition occurs for a critical coupling strength K_C satisfying $\lambda_j(K_C)=0$, and so given by

TABLE I. Values of the critical coupling strength for different lattice sizes and $\beta=3$.

N	K_{C1}	K_{C2}
3	$\frac{4}{9}$	$\frac{8}{9}$
19	$\frac{36}{57}$	$\frac{72}{57}$
57	$\frac{112}{171}$	$\frac{224}{171}$

$$K_C(\beta,N)=\begin{cases} K_{C1}\equiv a^*(N)\left(1-\frac{1}{\beta}\right) & \text{for } K_{C1}<a^*, \\ K_{C1}\equiv a^*(N)\left(1+\frac{1}{\beta}\right) & \text{for } K_{C2}>a^*, \end{cases} \tag{8}$$

where

$$a^*(N)\equiv 1+\frac{1}{N-1}, \tag{9}$$

showing that the critical coupling strength values for obtaining a chaos-hyperchaos transition depend both on β and the lattice size N, i.e., K_C is an extensive quantity. In the thermodynamic limit ($N\to\infty$) we have that a^* goes to unity. From now on we shall use $\beta=3$, such that $K_{C1}=\frac{2}{3}a^*(N)$ and $K_{C2}=\frac{4}{3}a^*(N)$. Their values for some lattice sizes are indicated in Table I.

The general aspects of the system dynamics can be understood from this point of view, as follows. For small enough values of the coupling strengths, i.e., $K<K_{C1}$, the maps are so weakly coupled that their chaotic evolutions are noncorrelated, and the system attractor is supposedly a high-dimensional set in the N-dimensional phase space of the coupled map system. As K crosses K_{C1}, however, since the Lyapunov spectrum presents a $(N-1)$-fold degeneracy, all but one Lyapunov exponent becomes positive for $K>K_{C1}$. In this case the chaotic maps synchronize, such that the system attractor collapses to the synchronization manifold, which is a one-dimensional subspace given by [22]

$$x_n(1)=x_n(2)=\cdots=x_n(N) \tag{10}$$

for any time n.

In fact, the synchronized state (10) exists for any value of the coupling strength K, for it is a valid solution of the coupled map lattice (5). If $K<K_{C1}$ it is not observed, however, because it is transversely unstable, i.e., the synchronized state is unstable under infinitesimal displacements along directions transversal to the synchronization manifold. In other words, if a synchronized state is actually observed, what happens for $K_{C1}<K<K_{C2}$, it is because of its transversal stability. By the same token, when $K=K_{C2}$ the synchronized state loses transversal stability and we return to a nonsynchronized, high-dimensional hyperchaotic attractor.

Hence, the hyperchaotic state refers to the nonsynchronized attractor for the coupled system, whereas the chaotic state is the synchronized one. This is a particular case of the chaos-hyperchaos transition, namely when there is a synchronization manifold for the coupled system. On the other hand, this is not an extremely stringent requirement. It is straightforward to derive necessary, albeit not sufficient conditions for the existence of a synchronized state [23]. Let us consider a general form of a coupled map lattice, for a state variable $x_n(i)$ at discrete time n and attached to the site $i=1,2,\ldots N$,

$$x_{n+1}(i)=\sum_j B_{ij}f(x_n(j))\equiv f(x_n(i))+\sum_j g_{ij}f(x_n(j)), \tag{11}$$

where the local dynamics is governed by the map $x\mapsto f(x)$, for $x\in[0,1]$, and g_{ij} are coupling coefficients. While the uncoupled state variables are always bound to the unit interval, for the coupled map lattice (11) in order to have $x(i)_n\in[0,1]$ for all maps and further times, the following necessary and sufficient conditions must hold for all i, j:

$$B_{ij}\geqslant 0 \quad \text{and } 0\leqslant\sum_{j=1}^{N}B_{ij}\leqslant 1, \tag{12}$$

which are satisfied, for example, by the piecewise linear map $f(x)=\beta x(\mathrm{mod}1)$. The synchronization manifold defined in (10) is invariant under the system dynamics if and only if the summation in the second of conditions (12) is the same for all rows of the matrix B_{ij}. In view of Eq. (11) this implies that $\Sigma_{j=1}^{N}g_{ij}=0$, which is fulfilled by a large number of coupling prescriptions, including Eq. (5) and other forms as well, like local and power-law couplings for example.

IV. RECURRENCE-BASED SIGNATURES OF THE CHAOS-HYPERCHAOS TRANSITION

The coupled map system can be regarded, at first, as a black-box, which would give us only the output of some map, like $x_n(2)$, as a function of discrete time n. This would be the analogue of the situation encountered by an experimenter when he (or she) is measuring some physical quantity from a supposedly complex system whose governing equations are poorly or not known in advance. We make recurrence plots of the time series so obtained for different values of K, in order to investigate when and how the chaos-hyperchaos transition occurs.

From Table I, in the case of $N=3$ coupled maps (with $\beta=3$), the values of K for which the chaos-hyperchaos transition occur are $K_{C1}\approx 0.44$ and $K_{C2}\approx 0.88$. The time series for values of K before the transition [Fig. 1(a)] and after [Fig. 1(b)] are hardly distinguishable. On the other hand, their corresponding recurrence plots do show some different characteristics, although a more precise characterization would need the use of recurrence quantification analysis.

Special emphasis has been put on the following quantifiers: (i) The recurrence rate (R_r), the determinism (D), the average diagonal length L, and the maximum diagonal length $\ell_{\max}$. All these quantities deal with the properties of diagonal

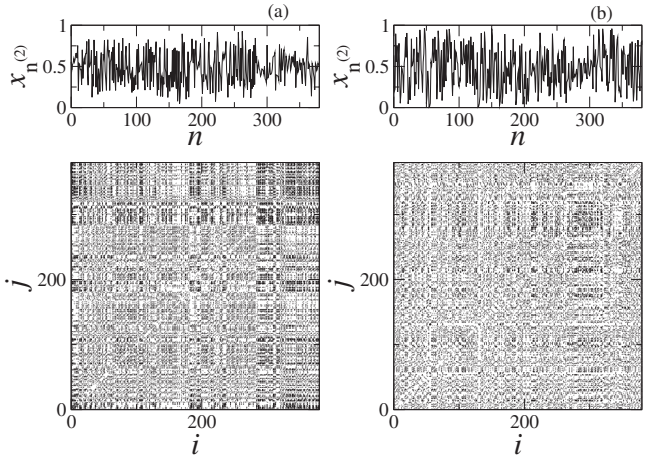

FIG. 1. Time evolution (top) and recurrence plots (bottom) of the variable $x_n(2)$ for a coupled map lattice with $\beta=3$, $N=3$ and (a) $K=0.3$ and (b) $K=0.8$. We have used an embedding dimension $d=1$ and delay $\tau=1$, with a cutoff radius equal to 0.01 times the phase-space diameter.

lines, since they measure our ability to detect the underlying determinism of the time series. Figure 2 shows the variation of these quantifiers with the coupling strength K for $N=3$ coupled maps.

The recurrence rate suffers a sudden increase exactly at the point K_{C1} when there is a transition from hyperchaos ($K<K_{C1}$) to chaos ($K>K_{C1}$) [Fig. 2(a)]. A more pronounced increase at the transition is exhibited by the determinism [Fig. 2(b)]. The observed decrease of determinism before the transition is basically a coupling effect, whereas the plateau observed after the transition is a consequence of the stationarity of the system, since it is now on the synchronization subspace.

Similar conclusions hold for the average diagonal length [Fig. 2(c)] and maximum diagonal length [Fig. 2(d)]. The common information conveyed by these quantifiers is that

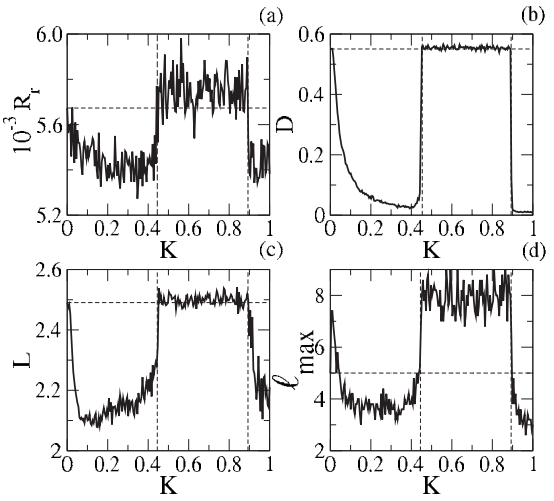

FIG. 2. Dependence of some recurrence quantifiers with the coupling strength for $N=3$ coupled map lattices with $\beta=3$: (a) recurrence rate; (b) determinism; (c) average diagonal length; (d) maximum diagonal length.

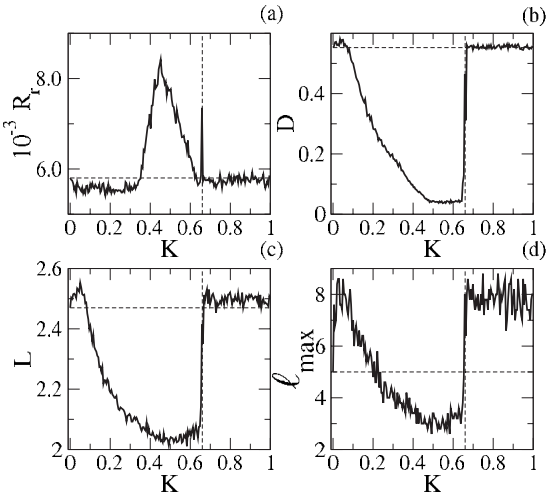

FIG. 3. Dependence of some recurrence quantifiers with the coupling strength for $N=57$ coupled map lattices with $\beta=3$: (a) Recurrence rate; (b) determinism; (c) average diagonal length; (d) maximum diagonal length.

the degree of determinism increases as the system goes from a large-dimensional and hyperchaotic attractor to a low-dimensional chaotic one, actually located at the synchronization manifold. This ability results from the strong contraction suffered by the system attractor when K crosses K_{C1}. Two neighbor trajectories, after the transition, are constrained to move strictly on the one-dimensional synchronization manifold, thus increasing the probability of having recurrences. From Fig. 2(a) this increase is very small (less than 8%) but nevertheless easily detectable, going approximately from 0.54% to 0.58% of recurrent events.

As we have seen in the preceding section, the chaos-hyperchaos transition point depends also on the lattice size, when a chaotic coupled map lattice is considered. We have verified this fact using recurrence quantification analysis, our results being depicted in Fig. 3. All quantifiers are shown to suffer a quite abrupt variation when K takes on its first critical value $K_{C1}=0.655$. Notice that the second critical value is not actually observed, since we have restricted the value of K to be less than the unity. The recurrence has the most distinctive behavior, for it presents a peak at K_{C1}, having been grown and decayed after this critical value [Fig. 3(a)]. This behavior, absent for a few coupled maps, is expected only for larger lattices, and the broad peak before the transition increases its height with N (Fig. 4). The large fluctuations for $N=19$ and $N=57$ are caused by an intermittent switching between states close to the synchronization subspace and nonsynchronized ones. This phenomenon has been called chaos-hyperchaos intermittency in Ref. [18].

The determinism, on the other hand, increases almost 50% and it is clearly an indicator of the transition from hyperchaos to chaos, thanks to the dramatic shrinking of the system attractor to just one phase-space dimension [Fig. 3(b)]; the other diagnostics leading to the same conclusion [Figs. 3(c) and 3(d)]. The attractor shrinking seems not to be uniform, as suggested by Fig. 5, where the bifurcation diagram in the synchronization manifold is presented for different lattice sizes. The hyperchaos-chaos transition coincides

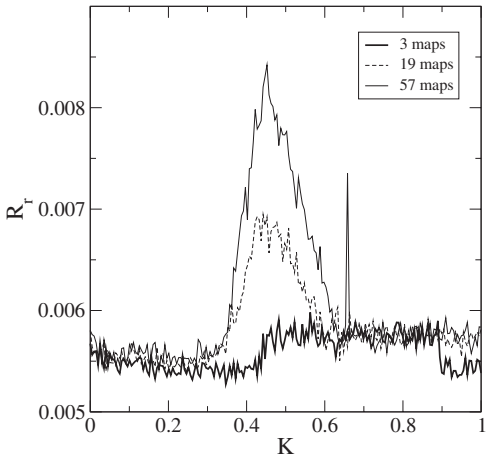

FIG. 4. Dependence of the recurrence with the coupling strength for different values of the lattice size.

with the value of K where the natural measure in the synchronization manifold extends over all of the [0, 1] interval. Since before this value the natural measure occupies a smaller interval this would mean that the shrinking of the system attractor occurs mainly in the transversal directions. Due to the large dimensionality of the phase space, however, this prediction is quite difficult to be directly verified.

So far in this paper we have used stationary time series (the parameters were kept fixed in the analyzed series). In order to demonstrate that our results can also be applied to a nonstationary time series, we have artificially created a nonstationary series from the deterministic evolution equations in the following way: We start our system using $K=0$ (uncoupled maps). We allow the system to stay with the same K value for Z time steps, where Z is an integer randomly (with uniform probability) chosen in the interval $2<Z<21$. After Z time steps, a new K value is calculated as $K_{\text{new}}=K+\Delta K$, where ΔK is a randomly chosen real number within the interval $10^{-6}<\Delta K<10^{-5}$. This procedure results in a time series with 2.2×10^6 points that is analyzed in blocks of 1000 points. We have used a window shift equal to 2, such that a large (998) number of points belonging to a block, belongs also to the following block and so on until the end of the entire time series. Figure 6 displays our results. As we can observe the transition from hyperchaos to chaos is still observed in the nonstationary series. Nevertheless the exact value of K for the transition is blurred by our procedure. Even so, a clear signature of the transition is still observable.

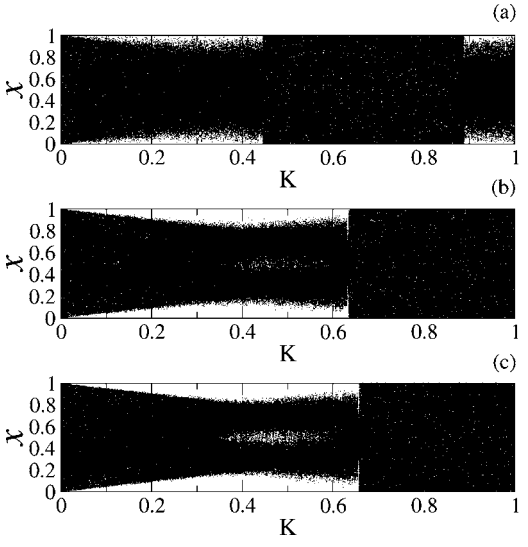

FIG. 5. Bifurcation diagrams in the synchronization manifold for different lattice sizes: (a) $N=3$; (b) $N=19$; (c) $N=57$. The sudden increase of the density of points coincides with the hyperchaos-chaos transition.

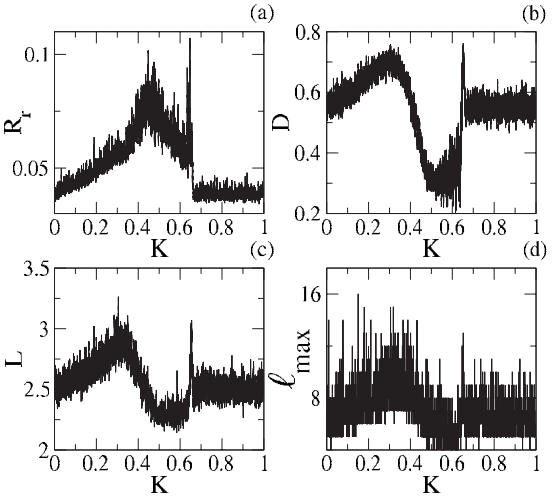

FIG. 6. Dependence of some recurrence quantifiers with the coupling strength for $N=3$ coupled map lattices with $\beta=3$ and K is randomly changed: (a) Recurrence rate; (b) determinism; (c) average diagonal length; (d) maximum diagonal length.

V. HYPERCHAOS-CHAOS TRANSITION IN COUPLED CHUA-MATSUMOTO CIRCUITS

In order to see the application of recurrence quantification analysis to locate the hyperchaos-chaos transition in a chaotic system of physical interest, we consider two coupled identical Chua-Matsumoto circuits [24]. Let (x_1,y_1,z_1) and (x_2,y_2,z_2) be the dimensionless dynamical variables for each circuit. The coupled system is then described by the following set of equations [18]:

$$\frac{dx_1}{dt}=\alpha[y_1-x_1-f(x_1)], \tag{13}$$

$$\frac{dy_1}{dt}=x_1-y_1+z_1+K(y_2-y_1), \tag{14}$$

$$\frac{dz_1}{dt}=-\beta y_1, \tag{15}$$

$$\frac{dx_2}{dt}=\alpha[y_2-x_2-f(x_2)], \tag{16}$$

$$\frac{dy_2}{dt}=x_2-y_2+z_2+M(y_1-y_2), \tag{17}$$

$$\frac{dz_2}{dt} = -\beta y_2, \tag{18}$$

where the piecewise-linear characteristic curve of each circuit is described by the normalized functions

$$f(x_1) = bx_1 + \tfrac{1}{2}(a-b)(|x_1+1| - |x_1-1|), \tag{19}$$

$$f(x_2) = bx_2 + \tfrac{1}{2}(a-b)(|x_2+1| - |x_2-1|), \tag{20}$$

where α, β, a, and b are constants. The specific type of coupling assumed here acts as a negative feedback on each circuit. In the following we shall consider the case in which the coupling is unidirectional, i.e., $M=0$ with $K\neq 0$, or a master-slave configuration.

In the following we choose the same parameter values as in Ref. [18], namely $\alpha=10.0$, $\beta=14.87$, $a=-1.27$, and $b=-0.68$, such that each circuit displays chaotic behavior when uncoupled, with a double-scroll chaotic attractor corresponding to the initial conditions $x_1(0)=0.010$, $x_2(0)=0.011$, $y_1(0)=z_1(0)=y_2(0)=z_2(0)=0$. The coupled system ($K\neq 0$) has a six-dimensional phase space where the synchronized state, given by the simultaneous conditions $x_1(t)=x_2(t)$, $y_1(t)=y_2(t)$, $z_1(t)=z_2(t)$, defines a three-dimensional synchronization subspace.

The Lyapunov spectrum is comprised of two sets of exponents: $\{\lambda_\parallel,\lambda_\perp\}$, where the first set, $\lambda_\parallel=\{\lambda_1,\lambda_2,\lambda_3\}$, contains the three ordered exponents related to the synchronized orbit. The second set of conditional (and ordered) Lyapunov exponents, $\lambda_\perp=\{\lambda_4,\lambda_5,\lambda_6\}$, is related to the directions transversal to the synchronization subspace. If the maximal transversal exponent is negative ($\lambda_4<0$) and the maximal parallel exponent is positive ($\lambda_1>0$) there is a chaotic attractor embedded in the synchronization subspace, whereas if $\lambda_4>0$ and $\lambda_1>0$ there is a hyperchaotic attractor. Fixing all parameters but increasing the coupling strength indicates that, at $K=K_c\approx 1.17$ the system attractor evolves from hyperchaos to chaos, following the transition from a nonsynchronized to a synchronized trajectory.

We have chosen the output $x_2(t)$ of the slave circuit as the time series to apply recurrence quantification analysis (similar results were obtained from the other variables of the slave circuit). In Fig. 7 we show the variation with the coupling strength of the four recurrence-based diagnostics already used for coupled maps. We observed a consistent increase of all after the transition takes place (indicated as a dashed line). In spite of the scales having been adjusted to ease of visualization, the most dramatic increase after the hyperchaos-chaos transition occurred with the determinism (which when augmented 3 times is the value after the transition), followed by the maximum diagonal length (which increase by 67%). Both the recurrence rate and the average diagonal length have an increase of about 10% of its value prior to the synchronization.

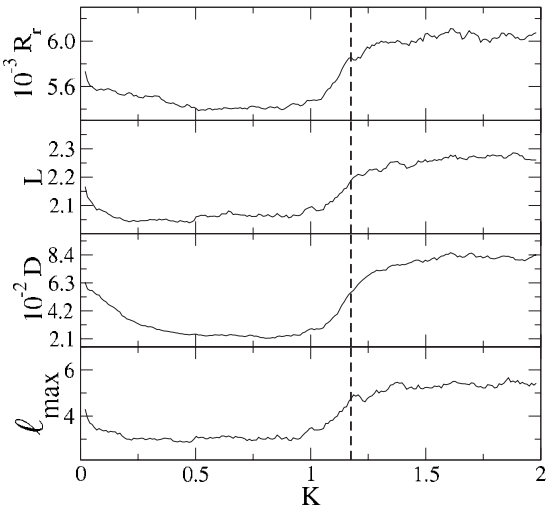

FIG. 7. Dependence of some recurrence quantifiers with the coupling strength for two unidirectionally coupled Chua-Matsumoto circuits using the same parameters as in Ref. [18] recurrence rate; (b) determinism; (c) average diagonal length; (d) maximum diagonal length. The dashed line indicates the hyperchaos-chaos transition.

VI. CONCLUSIONS

In this paper we have used the recurrence properties of chaotic trajectory to give a precise localization of the transition from a hyperchaotic to a chaotic attractor. Recurrence quantification analysis can act as a telescope in order to reveal the fine structure of a time series. We investigated this transition using coupled chaotic maps (using a global, or mean-field coupling scheme, where a system interacts with all other ones) and unidirectionally coupled Chua-Matsumoto circuits.

When the coupling strength is comparatively low, the dynamics occurs at a typically high-dimensional chaotic attractor, with more than one positive Lyapunov exponent (hyperchaos). As the coupling strength increases past a critical value (which we can predict analytically from the corresponding Lyapunov spectrum) the maps become synchronized and the attractor shrinks to a one-dimensional synchronization subspace, where there is only one positive Lyapunov exponent. Hence, the approach to a stable synchronization state marks also the hyperchaos-chaos transition.

Since, in the low-dimensional synchronized state, the trajectory is expected to present more recurrences than in a higher-dimensional chaotic attractor, the recurrence-based diagnostics present a significant increase as this transition takes place. This can be useful for describing chaos-hyperchaos transition from univariate time series coming from, e.g., measurements of some physical system behaving chaotically. We remark that usual characterization methods based on some form of phase-space reconstruction (as delay coordinates) fail to give an accurate description of the transition to hyperchaos, when it is known to occur.

Our results have confirmed in a clear-cut fashion the increase of recurrence properties following the transition to a synchronized state, but we think that similar results can be obtained even though the system does not present such a dramatic dimension shrinking as that occurring in our coupled map system. Hence, even though the physical system under consideration does not exhibit a synchronization

subspace or other low-dimensional submanifold where the chaotic attractor lies, we claim that the recurrence based diagnostics are sensitive enough to detect the dimensional reduction characteristic of a chaos-hyperchaos transition.

ACKNOWLEDGMENT

This work was partially supported by CNPq, CAPES, and Fundação Araucária (Brazilian agencies).

[1] O. E. Rössler, Phys. Lett. **71A**, 155 (1979).
[2] P. Colet, R. Roy, and K. Wiesenfeld, Phys. Rev. E **50**, 3453 (1994); L. Yang, Z. Liu, and J. Mao, Phys. Rev. Lett. **84**, 67 (2000).
[3] T. Matsumoto, L. O. Chua, and K. Kobayashi, IEEE Trans. Circuits Syst. **33**, 1143 (1986).
[4] R. Stoop and P. F. Meier, J. Opt. Soc. Am. B **5**, 1037 (1988).
[5] R. Stoop, J. Peinke, J. Parisi, B. Röhricht, and R. P. Huebener, Physica D **35**, 425 (1989).
[6] M. Eiswirth, Th.-M. Kruel, G. Ertl, and F. W. Schneider, Chem. Phys. Lett. **193**, 305 (1992).
[7] T. Kapitaniak, K. E. Thylwe, I. Cohen, and J. Wojewoda, Chaos, Solitons Fractals **5**, 2003 (1995).
[8] H. Kantz and T. Schreiber, *Nonlinear Time Series Analysis* (Cambridge University Press, Cambridge, 1997).
[9] C. Letellier and L. A. Aguirre, Chaos **12**, 549 (2002).
[10] M. Casdagli, Physica D **108**, 12 (1997).
[11] F. Takens, in *Dynamical Systems and Turbulence*, edited by D. A. Rand and L. S. Young, Springer Lecture Notes in Mathematics, 898 (Springer-Verlag, New York, 1980).
[12] J.-P. Eckmann, S. O. Kamphorst, and D. Ruelle, Europhys. Lett. **4**, 973 (1987).
[13] J. P. Zbilut and C. L. Webber, Jr., Phys. Lett. A **171**, 199 (1992).
[14] N. Marwan, M. C. Romano, M. Thiel, and J. Kurths, Phys. Rep. **438**, 237 (2007).
[15] C. L. Webber, Jr. and J. P. Zbilut, J. Appl. Physiol. **76**, 965 (1994).
[16] M. Thiel, M. C. Romano, P. L. Read, and J. Kurths, Chaos **14**, 234 (2004).
[17] M. Thiel, M. C. Romano, and J. Kurths, Appl. Nonlinear Dyn. **11**, 20 (2003).
[18] V. S. Anishchenko, T. Kapitaniak, M. A. Safonova, and O. V. Sosnovzeva, Phys. Lett. A **192**, 207 (1994).
[19] R. L. Devaney, *An Introduction to Chaotic Dynamical Systems* (Benjamin-Cummings, Reading, PA, 1986).
[20] T. Shimada and K. Kikuchi, Phys. Rev. E **62**, 3489 (2000).
[21] A. M. Batista, S. E. de S. Pinto, R. L. Viana, and S. R. Lopes, Phys. Rev. E **65**, 056209 (2002).
[22] L. M. Pecora and T. L. Carroll, Phys. Rev. Lett. **64**, 821 (1990).
[23] R. L. Viana, C. Grebogi, S. E. de S. Pinto, S. R. Lopes, A. M. Batista, and J. Kurths, Physica D **206**, 94 (2005).
[24] T. Matsumoto, IEEE Trans. Circuits Syst. **31**, 1055 (1984); T. Matsumoto, L. O. Chua, and M. Komuro, *ibid.* **32**, 797 (1985).